Covalent chemical functionalization of semiconducting layered chalcogenide nanosheets

Journal:	*Molecular Systems Design & Engineering*
Manuscript ID	ME-ART-04-2019-000045.R1
Article Type:	Paper
Date Submitted by the Author:	04-Jun-2019
Complete List of Authors:	Li, Duo; Arizona State University, Materials Science and Engineering Gilliam, Matthew; Arizona State University, School of Molecular Sciences; Arizona State University, Biodesign Institute Chu, Ximo; Arizona State University, Materials Science and Engineering Yousaf, Ahmed; Arizona State University, School of Molecular Sciences; Arizona State University, Biodesign Institute Guo, Yuqi; Arizona State University, Materials Science and Engineering Green, Alexander; Arizona State University, School of Molecular Sciences; Arizona State University, Biodesign Institute Wang, Qing Hua; Arizona State University, Materials Science and Engineering

Covalent chemical functionalization of semiconducting layered chalcogenide nanosheets

Duo O. Li[1], Matthew S. Gilliam[2,3], Ximo S. Chu[1], Ahmed Yousaf[2,3], Yuqi Guo[1], Alexander A. Green[2,3], and Qing Hua Wang[1]*

1. Materials Science and Engineering, School for Engineering of Matter, Transport and Energy, Arizona State University, Tempe, AZ, 85287
2. School of Molecular Sciences, Arizona State University, Tempe, AZ, 85287
3. Biodesign Center for Molecular Design and Biomimetics, The Biodesign Institute, Arizona State University, Tempe, AZ, 85287

* Corresponding author: qhwang@asu.edu

Abstract

Layered chalcogenides are a diverse class of crystalline materials that consist of various covalently bound building blocks held together by van der Waals forces. Among these materials are the transition metal dichalcogenides (TMDCs) which can be exfoliated into two-dimensional (2D) nanosheets, and the pnictogen chalcogenides (PCs) which can be exfoliated into one-dimensional (1D) nanoribbons and 2D nanosheets. These materials have recently been extensively studied for their intriguing electronic, optical, and chemical properties. The chemical functionalization of 1D and 2D nanomaterials is an important enabling step for tuning their properties and forming interfaces with other materials and structures. However, broadly applicable and versatile chemical tools that can effectively functionalize a wide range of layered chalcogenide compositions without disruptive pre-treatments need further advancement. Here we show the covalent functionalization of nanosheets of the representative TMDC materials MoS_2, WS_2, $MoSe_2$, and WSe_2, and of the representative PC materials Sb_2S_3 and Bi_2S_3 using aryl diazonium salts. Covalent bonds are formed on the basal planes of both mechanically exfoliated and liquid phase dispersed nanosheets, and the chemical and morphological changes upon functionalization are verified using a combination of spectroscopic and microscopic techniques. This work builds on previous demonstrations of diazonium functionalization of 2D materials like MoS_2, and expands it to five additional compositions. Thus, the aryl diazonium chemistry is shown to be a versatile and powerful approach to covalent functionalization of the 2D nanosheets of a diverse set of semiconducting layered chalcogenide materials.

Design, System, Application

Due to their high aspect ratios and extreme thinness, 2D materials are sensitive to modifications via chemistry on their surfaces. The study of 2D materials in recent years has encompassed a broad range of crystalline materials of different compositions and properties, which have also required developing different chemical modification schemes. Covalent functionalization of the basal planes of 2D materials is more robust and stable than non-covalent modification, and allows for stronger effects on the properties of the target 2D materials. However, covalent modification is also more likely to alter or disrupt the intrinsic crystal structure of 2D materials and lead to undesirable changes in properties. In this work, we demonstrate the covalent functionalization of several different compositions of layered semiconducting chalcogenide materials using aryl diazonium salts without disrupting their crystal structures. The materials are MoS_2, WS_2, $MoSe_2$, WSe_2, Sb_2S_3 and Bi_2S_3. The successful covalent attachment of molecular groups on these 2D materials is confirmed using vibrational spectroscopy, and their spatial distribution across the surfaces is imaged with atomic force microscopy. These results show that the diazonium functionalization is broadly applicable to several types of layered chalcogenides. There is potential to further exploit this chemistry to form linkages and interfaces with other materials and structures for applications in electronics and sensors.

Introduction

Over the past decade, the study of 2D materials that can be derived from layered bulk materials with in-plane covalent bonding and out-of-plane van der Waals (vdW) bonding has been intensely pursued due to their unique electronic, optical, mechanical, and chemical properties, and in particular the layered chalcogen materials have attracted significant attention. One important class of such materials are the transition metal dichalcogenides (TMDCs), which have the general formula MX_2, where M is a transition metal (M = Mo, W, Nb, Ta, etc.) and X is a chalcogen (X = S, Se, or Te). Members of the TMDC family include metallic, semiconducting, superconducting, charge density wave, and topological materials, and have recently been the focus of intense research efforts due to the unique properties that arise in their 2D forms.[1–4] They have been used in a wide range of applications in electronics, sensing, and energy.[5–7] The crystal structure of the MX_2 materials including the semiconductors MoS_2, $MoSe_2$, WS_2, and WSe_2, which belong to the *$P6_3/mmc$* space group (No. 194) in their most common phases, is shown in **Figure 1a-b**. These materials have covalently bound layers with either S or Se atoms on the outer planes that are held in stacks by vdW forces.

The pnictogen chalcogenides (PCs) are another class of layered chalcogens, with the general formula Pn_2X_3, where Pn is a group 15 pnictogen (Pn = As, Sb, and Bi). While the broader group includes semiconductors, topological insulators, and thermoelectrics, here in this paper we focus on the

semiconductors Sb_2S_3 and Bi_2S_3. These materials have been grown in thin films,[8] nanowires and nanorods,[9–14] and exfoliated into 1D nanoribbons and 2D nanosheets.[15–17] Examples of applications for Bi_2S_3 and Sb_2S_3 include solar cells, batteries, and catalysts.[9,10,17–20] The crystal structure of the Pn_2X_3 materials including Sb_2S_3 (antimony trisulfide or antimonite or stibnite) and Bi_2S_3 (bismuth(III) sulfide or bismuthinite), which belong to the *Pnma* space group (No. 62), are shown in **Figure 1c-d**.

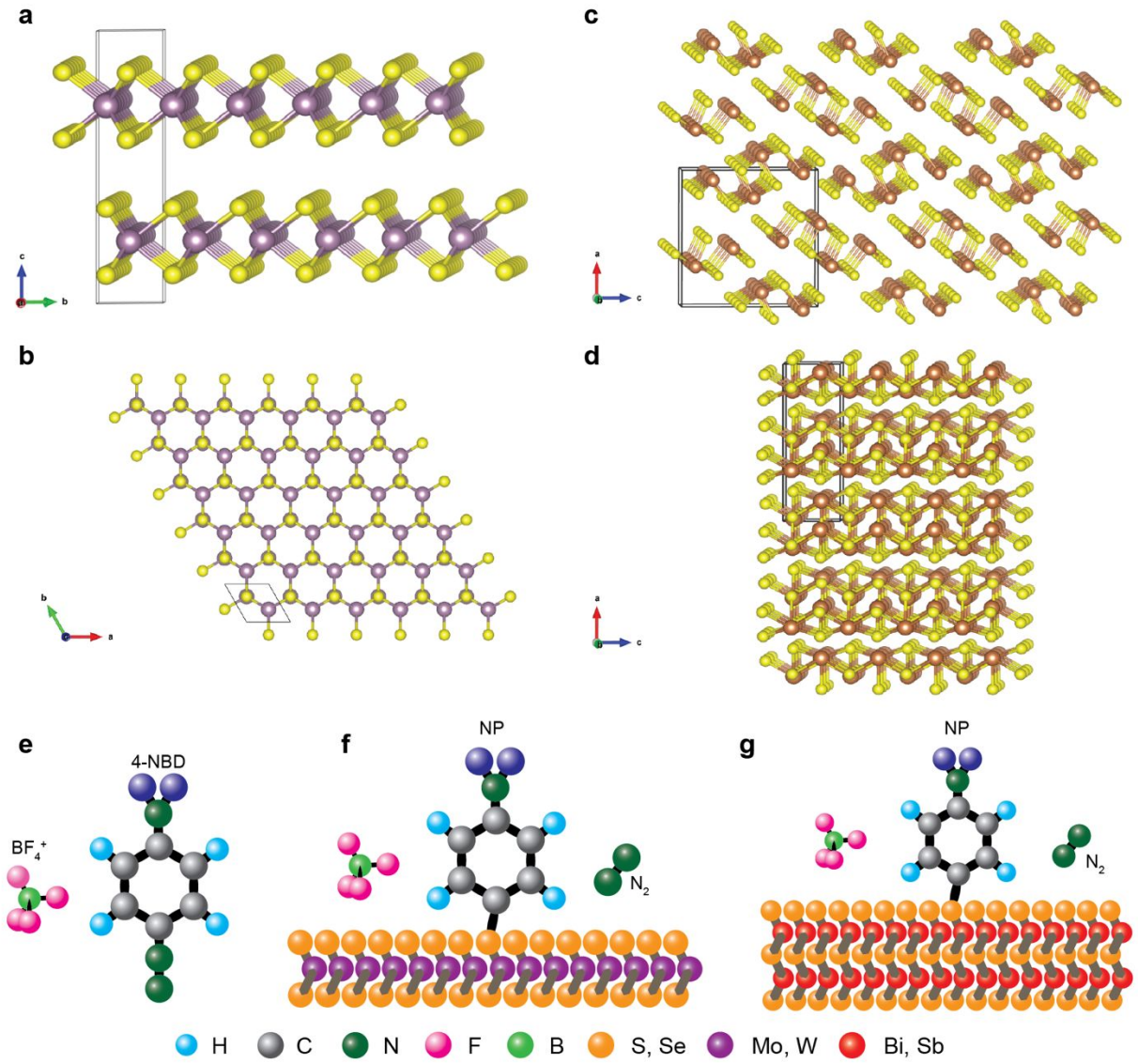

Figure 1. Layered chalcogenide materials and diazonium functionalization scheme. (a)-(b) Crystal structure of MX_2 materials in side and top views (yellow atoms: X; purple atoms: M). (c)-(d) Crystal structures of Pn_2X_3 materials in side and top views (yellow atoms: X; brown atoms: Pc). (e)-(g) Reaction scheme for covalent functionalization with aryl diazonium salts: (e) the functionalization is done using 4-nitrobenzenediazonium tetrafluoroborate (4-NBD), which forms a radical upon charge transfer from the substrate; the radical forms a covalent bond with the S or Se atom at the surface; and (f)-(g) there is a covalently bonded nitrophenyl (NP) group on the surface as a result.

The chemical functionalization of nanomaterials is used to tune their physical properties, control their interfacial interactions with other materials, and to protect them from deleterious environments. In general, 2D materials like graphene can be functionalized by both covalent and non-covalent methods.[21–23] For example, the surface functionalization of TMDCs can allow them to have improved biosensing capabilities by introducing biophilic moieties to bind particular biomolecules,[24–26] better antimicrobial activity,[27,28] sorption of contaminants from water,[29] and doping of the semiconducting material.[30]

Recently, we have demonstrated the direct covalent functionalization of semiconducting 2D MoS_2 by aryl diazonium salts,[31] which does not require any pre-treatment or phase conversion of the semiconducting material, and we have also shown the detailed reaction kinetics of this functionalization,[32] which depends on the energetically inhomogeneous surface due to defects and the interaction between the attached NP groups on the surface and the free 4-NBD molecules in solution. Aryl diazonium functionalization has previously been applied to other materials such as graphene,[22,23,33,34] black phosphorus,[35] and carbon nanotubes.[36] The TMDCs, in particular MoS_2, have been the focus of several surface functionalization studies,[25,37,38] and a variety of approaches and chemical schemes have been used.[26,38–44] Many of these methods require lithium-based phase conversion or the formation of defects. There have also been some examples of surface functionalization for the PCs,[45–48] but there are fewer such methods for PCs than for TMDCs to the best of our knowledge. Thus, there is a need for a general and broadly applicable method to functionalize different layered chalcogenides, and in particular to expand them to the PCs.

In this paper, we expand this covalent functionalization with aryl diazonium salts to several other members of the TMDC and PC families beyond MoS_2 to further extend the applicability and broad utility of this chemistry, namely to functionalize $MoSe_2$, WS_2, WSe_2, Bi_2S_3, and Sb_2S_3. We prepare and functionalize samples of these materials using mechanical exfoliation, liquid phase dispersion, and chemical vapor deposition (CVD) techniques. Using vibrational and absorbance spectroscopies, we show the formation of chemical bonds and attachment of functional groups to the TMDC and PC nanosheets. Using atomic force microscopy (AFM), we show the spatial distribution of NP groups across the TMDC and PC surfaces with functionalization. This work shows that the covalent functionalization using aryl diazonium salts can indeed be applied to many related layered chalcogen materials, thus greatly expanding the scope of utility of the chemical scheme, and that it can open the door to further modifications of these materials. Our generalized approach for both TMDCs and PCs here uses diazonium chemistry to produce surface-modified nanomaterials that opens avenues for potential applications in biosensing, antimicrobial, therapeutic, environmental, energy, and optoelectronic applications. The winder literature on the diazonium functionalization of 2D materials and carbon nanomaterials, which has demonstrated changes to properties such as the electronic and transport,[49] shifts in optical emission,[31] and the covalent attachment of other materials[23,31,33] like proteins, polymers, and quantum dots, can be brought to inform future work on TMDCs and PCs.

Experimental

Materials

Tungsten (IV) sulfide (WS_2, powder, 99%, 2 μm), molybdenum (IV) selenide ($MoSe_2$, ~325 mesh, 99.9% trace metals basis), molybdenum(IV) sulfide (MoS2, powder), bismuth (III) sulfide (Bi_2S_3, 99%), antimony (III) sulfide (Sb_2S_3, powder), 4-nitrobenzenediazonium tetrafluoroborate (4-NBD, 97%), sodium dodecyl sulfate (SDS, BioReagent, suitable for electrophoresis, for molecular biology, ≥98.5% GC), molybdenum (VI) oxide (MoO_3), and selenium (Se powder) were purchased from Sigma-Aldrich. Tungsten (IV) selenide (WSe_2, 10-20 μm powder, 99.8% metals basis) and sulfur (S powder) were purchased from Alfa Aesar. Single crystals of MoS_2 and WS_2 were purchased from SPI Supplies, $MoSe_2$ from MTI Corporation, and WSe_2 from Nanosurf.

Mechanical exfoliation

Si/SiO_2 (300 nm) substrates were ultrasonically cleaned in acetone and isopropanol baths sequentially and then blown dry with ultrahigh purity nitrogen gas. The TMDC flakes were prepared by mechanical exfoliation from single crystals, while the PC flakes were prepared by using the same method from bulk powders.

Liquid phase exfoliation

Liquid exfoliation for TMDCs and PCs used bulk powder source materials mixed in 1% wt/vol SDS aqueous solutions and subjected to tip sonication (Branson Digital Sonifier 450D) with a 3 mm tip for 2-4 hours at 30-50% amplitude. The mixtures were then centrifuged for 5-30 min at 3234 to 5000 RCF and the supernatant containing the dispersed nanosheets were extracted and used for further experiments. The masses, sonication times and amplitudes, and centrifugation times and speeds for each material are as follows: MoS_2 according to methods in Chu et al.;[31] WS_2: 5 g in 110 mL SDS solution, 2 hours at 50% amplitude, 30 minutes at 3234 RCF; $MoSe_2$ and WSe_2: 0.65 g in 20 mL SDS solution, 2 hours at 30% amplitude; Bi_2S_3 and Sb_2S_3: 1.3 g each in 20 mL SDS solution, 4 hours at 35% amplitude, 5 minutes at 5000 RCF.

Functionalization of mechanically exfoliated samples

The mechanically exfoliated flakes of TMDCs and PCs deposited on Si/SiO_2 were immersed in 10 mM of 4-nitrobenzenediazonium tetrafluoroborate (4-NBD) (Sigma Aldrich) aqueous solutions at 35°C with stirring at 125 rpm. The reaction was conducted in a beaker sealed by parafilm in the dark. Then the samples were removed from the solution and thoroughly rinsed with ultrapure water and blown dry with ultrahigh purity nitrogen gas.

Functionalization of liquid phase exfoliated samples

Nanosheet dispersions of each material were mixed with 4-NBD powder such that the concentration of 4-NBD was 0.25% wt/vol with respect to the nanosheet dispersion volumes. The mixtures were then subjected to tip sonication at 20% amplitude for 2 hours for MoS_2, WS_2, $MoSe_2$, and WSe_2 and for 4 hours for Bi_2S_3 and Sb_2S_3. Control samples were prepared by subjecting the nanosheet dispersions to the same sonication treatment but without any 4-NBD.

Raman spectroscopy

Raman spectroscopy and optical microscopy of mechanically exfoliated nanosheets of TMDCs and PCs were obtained on a WITec alpha300R system confocal Raman microscope system with a 532 nm excitation laser and 100X objective lens with ~1 μm laser spot size. The laser power was kept below 1 mW to minimize damage to the samples. Spectra were obtained using the 1800 g/mm grating and 5 s acquisition time.

Atomic force microscopy (AFM)

AFM images of mechanically exfoliated nanosheets were taken after different reaction times using a Multimode V system (Bruker Inc.) in ScanAsyst mode with ScanAsyst-Air tips (tip diameter 2 nm). AFM images were processed using Gwyddion.[50]

Fourier transform infrared spectroscopy (FTIR)

Nanosheet dispersions of all the TMDCs and PCs in both functionalized and unfunctionalized states were used to make thin films by vacuum filtration onto hydrophilic PTFE membranes (0.1 μm pore size, OMNIPORE, from Millipore) followed by washing with water and vacuum drying between 60 and 90°C overnight in a vacuum oven. Transmittance FTIR measurements were performed on the vacuum filtered films using a Nicolet 6700 FTIR with 64 scans taken for each sample and 128 scans taken for a background measurement in air. Within the OMNIC software used to collect the spectra, transmittance measurements were converted to absorbance measurements and a baseline correction was applied to each spectrum. The absorbance spectra were then normalized to a peak corresponding to PTFE that occurs at around 1150 cm^{-1} and plotted using MATLAB.

UV-vis absorbance spectroscopy (UV-vis)

Nanosheet dispersions were added to plastic cuvettes and their absorbance spectra were measured using a Jasco V-670 Spectrophotometer with 1% SDS solution as a baseline and reference. All dispersions and solutions were measured in plastic cuvettes.

Transmission electron microscopy (TEM)

Nanosheet dispersions were dropped onto 400 mesh Cu lacey carbon grids (01824 from Ted Pella) and imaged using a Philips CM 12 TEM operating at 80 kV.

Chemical vapor deposition (CVD)

The MoS_2 and $MoSe_2$ samples for XPS analysis were prepared using chemical vapor deposition (CVD) growth in a 1-inch quartz tube in a tube furnace (ThermoFisher Scientific). The target substrates were SiO_2/Si wafers held above the MoO3 precursors. During the growth of MoS_2, 20 mg of MoO_3 was heated up to 650ºC in 40 min and held for 30 min. 100 mg of S (Alfa Aesar) was separately heated up to 150ºC at an upstream location. The system was in vacuum with a 300 sccm of Ar flow. During the growth of $MoSe_2$, the growth was conducted in atmospheric pressure. The system was purged with a 500 sccm of Ar flow for 30 min before heating. 30 mg of MoO_3 was heated up to 150ºC and held for 30 min followed by heating up to 950ºC in 15 min and holding for 10 min. 200 mg of Se (Sigma-Aldrich) was separately heated up to 200ºC at an upstream location.

X-ray photoelectron spectroscopy (XPS)

XPS analysis was conducted using a Vacuum Generators 220i-XL system with monochromated Al Kα radiation (hv = 1486.6 eV). The pressure in the analysis chamber was ~10^{-9} torr or lower and the X-ray spot size was ~400 μm. The spectra were analyzed using the CasaXPS software package.

Results & Discussion

Chemical functionalization by aryl diazonium salts

The 2D nanosheets of TMDCs and PCs were prepared by mechanical exfoliation onto SiO_2/Si wafer substrates, by liquid phase exfoliation in aqueous surfactant solutions by tip sonication from powders, and by chemical vapor deposition (CVD) (see Experimental section for more details). The nanosheets were then covalently functionalized in aqueous solutions of the aryl diazonium salt 4-nitrobenzenediazonium tetrafluoroborate (4-NBD). This molecule, along with other similar derivatives, has been previously used to functionalize graphene[34,51] and MoS_2.[31,32] By choosing a molecule that has been used before, we can more directly compare the results for different substrate nanomaterials without concern over variables in reactivity or morphology that may occur in different diazonium derivatives.[52] The functionalization reaction proceeds as illustrated in the steps in **Figure 1e-g**, resulting in covalent C-S and C-Se bonds on the basal planes with nitrophenyl (NP) groups protruding from the surface. This reaction for MoS_2 alone was studied in greater detail in our previous work in Chu et al.[31] and Li et al.,[32] which confirmed the reaction mechanism and kinetics. Briefly, the reaction involves the transfer of charge from the target substrate material (MoS_2 in the case of the earlier work, and other TMDCs and PCs in the present work) to the aryl diazonium group, which forms an aryl radical upon loss of a nitrogen molecule, which then forms a covalent bond with the

basal plane. Our earlier work showed that the reaction mechanism relies on the presence of a very small concentration of sulfur vacancies in MoS_2 at which the local charge density is increased in order to initiate the reaction, which then progresses across the surface in a chain-like morphology due to the increased reactivity surrounding covalently functionalized sites.[31] Thus, only a very low number of initial defects was needed for the entire basal plane to be functionalized.

The mechanically exfoliated samples in the current study enabled careful imaging by AFM to observe the formation of covalently attached chemical groups on the nanosheets' surfaces with high spatial resolution, while the liquid phase exfoliated materials provided larger quantities of nanosheets that were suitable for ensemble measurements. Both types of samples and measurements are important for characterizing the overall functionalization of this collection of TMDC and PC layered materials.

Spectral evidence of chemical functionalization

Optical spectroscopy was used to characterize the functionalized and unfunctionalized TMDC and PC materials. For Fourier transform infrared spectroscopy (FTIR), films of nanosheets dispersed by liquid phase exfoliation were formed by vacuum filtration onto PTFE membranes (see Experimental section for more details). For and UV-visible absorbance spectroscopy, the nanosheet dispersions were directly measured in their liquid state. For Raman spectroscopy, mechanically exfoliated flakes were used.

The FTIR results for the TMDCs are shown in **Figure 2a**. The spectra for all the functionalized nanosheets show features around 1344 cm^{-1} and 1514 cm^{-1} corresponding to the N-O stretching modes, which indicates the presence of the NO_2 group from 4-NBD. There is also a peak at ~1600 cm^{-1} which can be associated with the C=C stretch within the benzene group of an attached nitrophenyl group resulting from the 4-NBD molecule. There is also a peak at 697 cm^{-1} corresponding to the C-S bond, although it is less prominent in some of the materials, possibly due to variations in film thickness. The C-Se bond is expected to occur at about ~640 cm^{-1},[43,44] but that is a busy part of the spectrum for $MoSe_2$, and is too weak to be clear for WSe_2 (although the N-O peaks are also weak in WSe_2). The FTIR spectra for the PCs are shown in **Figure 2b**. The same peaks for N-O stretching modes and the C=C stretch can clearly be seen in the 4-NBD treated PC samples, which also suggests the successful functionalization of PC materials. The presence of the C-S peak also indicates formation of covalent bonds on the PC surfaces. All these relevant peaks indicating successful functionalization are indicated by arrows.

Raman spectroscopy was conducted to verify that no significant structural change or damage occurs due to the 4-NBD functionalization reaction. Nanoflakes of TMDCs and PCs were prepared by mechanical exfoliation from bulk crystals and bulk powders, respectively, and deposited onto SiO_2/Si wafers, and identified with the optical microscope in the Raman system. As shown in **Figure S1** of the Electronic Supporting Information, the E^1_{2g} in-plane and A_{1g} intra-plane vibrations are detected both before and after functionalization, with no significant changes. The PC materials behave similarly, as shown in **Figure S2** of the Electronic Supporting Information, with the characteristic vibrations indicated. This finding

is important because it shows that the covalent attachment enables chemical modification to be conducted on the outer basal plane without significant disruption of the basic crystal structure of these materials.

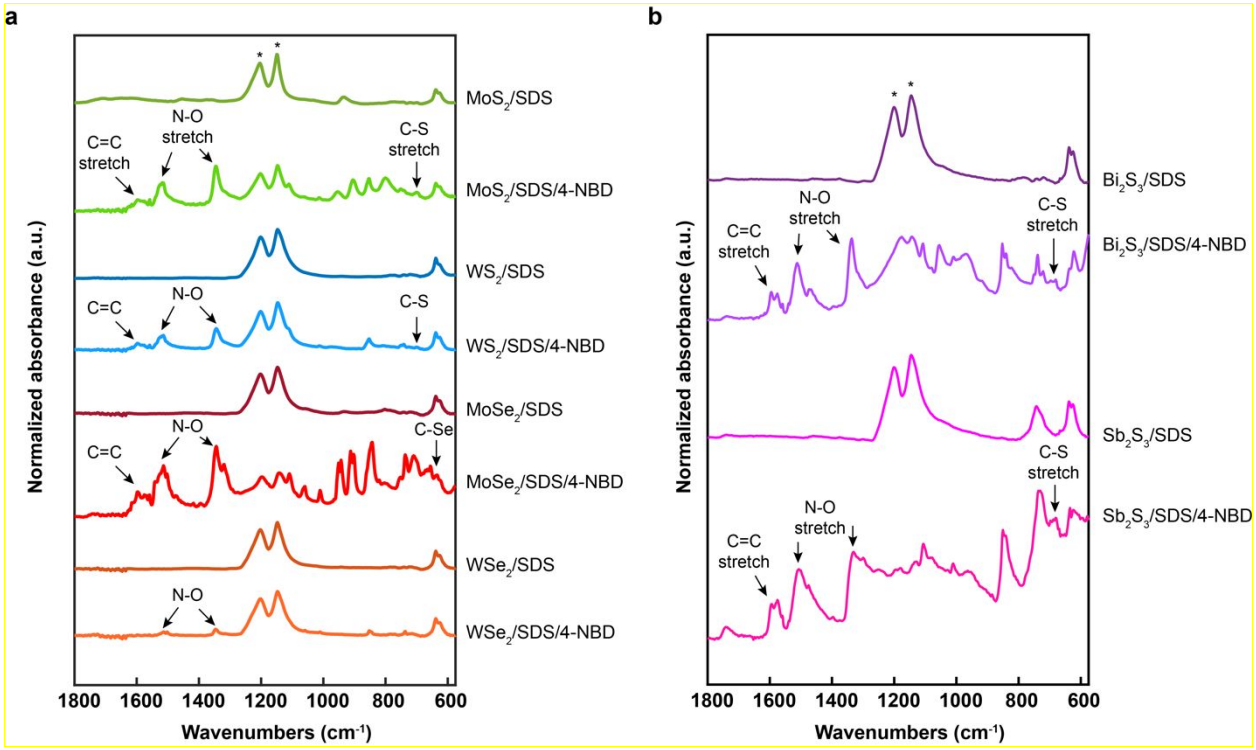

Figure 2. Vibrational spectroscopy for functionalized TMDCs and PCs from Fourier transform infrared spectroscopy (FTIR). Spectra for untreated and 4-NBD treated materials show a primary difference in the presence of an N-O stretch and C=C stretch in the treated samples, suggesting the presence of NO_2 and benzene groups and therefore a successful functionalization. The C-S and C-Se peaks associated with forming bonds at the surfaces of TMDCs and PCs are also present. The important peaks are indicated with arrows in the spectra for all the functionalized materials. The peaks from the PTFE support are indicated by asterisks (*).

Optical absorbance spectroscopy (UV-vis) was conducted to characterize the changes to the excitonic structure of the TMDC and PC materials. Samples were prepared by diluting dispersions of the nanosheets with 1% SDS solution so that their absorbance values were within the instrument's detection range (see Experimental section for more details). The UV-vis spectra for the TMDCs in **Figure 3a** show the characteristic excitonic peaks for MoS_2, WS_2, $MoSe_2$ and WSe_2 marked with asterisks. After 4-NBD functionalization, there is a slight red shift in these peaks, similar to our observations for MoS_2 in our previous work.[31] We attributed these shifts to the electronic coupling of excitons to the aromatic groups that are attached to the TMDC surfaces, which is similar to the excitonic redshift in functionalized CdSe quantum dots,[53] rather than due to an increase in layer thickness,[54] because the surface functionalization prevents proper restacking. The UV-vis spectra for PCs in **Figure 3b** are essentially featureless before and after

functionalization, as there are no excitonic peaks in this range, but there is some increase in the background below 500 nm due to absorbance of the 4-NBD for the functionalized materials.

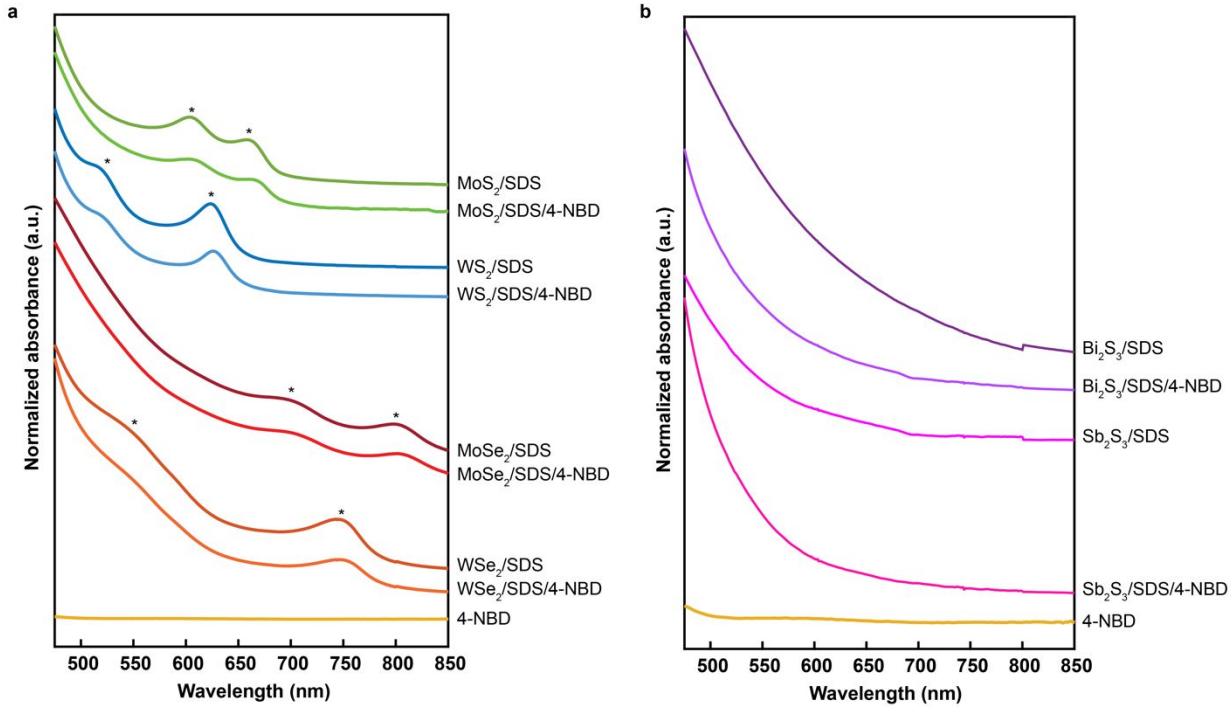

Figure 3. Absorbance spectroscopy for functionalized TMDCs and PCs. UV-vis spectra are shown vertically offset for (a) TMDCs and (b) PCs as-dispersed in SDS and with 4-NBD functionalization. The reference spectrum for 4-NBD is also shown in each panel. Asterisks (*) denote exciton peaks for TMDCs, which are slightly red-shifted after 4-NBD functionalization. The PC spectra are relatively featureless.

X-ray photoelectron spectroscopy (XPS) was conducted for $MoSe_2$ and MoS_2 to characterize the surface chemistry, as shown in **Figure S3** of the Electronic Supporting Information. After treating the samples with 4-NBD, clear N-O and N-C peaks due to the NO_2 groups appear and the intensities of the C peaks due to the benzene ring also increase, all indicative of successful functionalization with nitrophenyl groups. These changes in peaks are only known to appear when there is successful covalent functionalization with a molecule containing the diazonium-group, and are not seen for physisorption with the non-diazonium nitrobenzene molecule.[55,31] Further discussion of other features in the XPS spectra are in found the Electronic Supporting Information.

Morphology of functionalized layered chalcogenide materials

The morphologies of the TMDCs and PCs upon functionalization were characterized by AFM and TEM imaging on mechanically exfoliated and liquid phase exfoliated samples, respectively. AFM imaging is particularly valuable here to directly show the attachment of organic groups on the surfaces of the TMDCs and PCs, and was previously used in our earlier work to elucidate reaction mechanisms and kinetics by analyzing the change in surface coverage on MoS_2.[31,32] The AFM images of as-exfoliated and functionalized

TMDCs are shown in **Figure 4**. The thickness of the flakes ranges from 1 to 2 nm and corresponds to atomically thin monolayers and bilayers as shown in **Figure 4a-d**. After 5 s reaction in 4-NBD aqueous solution, small protrusions are observed on all the MoS_2, $MoSe_2$, WS_2 and WSe_2 flakes as shown in **Figure 4e-h**. The protrusions can be more clearly seen in the zoomed-in images in **Figure 4i-l**, which are from the areas highlighted by squares in **Figure 4e-h**. The heights of the protrusions range from 1 to 2 nm which is observed from height profiles shown in **Figure 4m-p**. The protrusions can be attributed to the nitrophenyl groups covalently attached onto the surfaces of the TMDCs nanosheets after reaction in 4-NBD aqueous solution. In addition, many of the protrusions are arranged in chain-like features are also observed on all the TMDCs because the attachment of 4-NBD molecules tend to propagate near the previously attached molecules, as found in our previous work on MoS_2 in Chu et al.[31] and Li et al.[32] which are also included in **Figure 4**. Physisorption is not expected to be a significant contribution because the samples were rinsed thoroughly with ultrapure water, and we previously showed in Chu et al. via a control reaction with a molecule that lacks the diazonium group to form the covalent reaction that very little physisorption occurs.[31]

AFM images of Bi_2S_3 and Sb_2S_3 flakes mechanically exfoliated from bulk powders are shown in **Figure 5**. The initial unreacted surfaces are shown in **Figure 5a-b**, where there are numerous atomic step edges visible, which tend to form ribbon-like features due to the presence of 1D chains in the crystal structure (see **Figure 1c-d**). The same regions of the samples are then shown after functionalization in **Figure 5c-f** (the asterisks indicate features that appear both before and after functionalization to help guide the eye), where there are many protrusions uniformly covering the surfaces. The appearance of these protrusions is very similar to those that appear on TMDCs in **Figure 4**. There are some clusters observed in **Figure 5f** and the height ranges from 1-4 nm which is similar to our earlier results in Li et al.[32] Thus, the PC materials and TMDC materials possess similar morphology after functionalization, suggesting consistent attachment of organic groups to the surfaces are 4-NBD treatment.

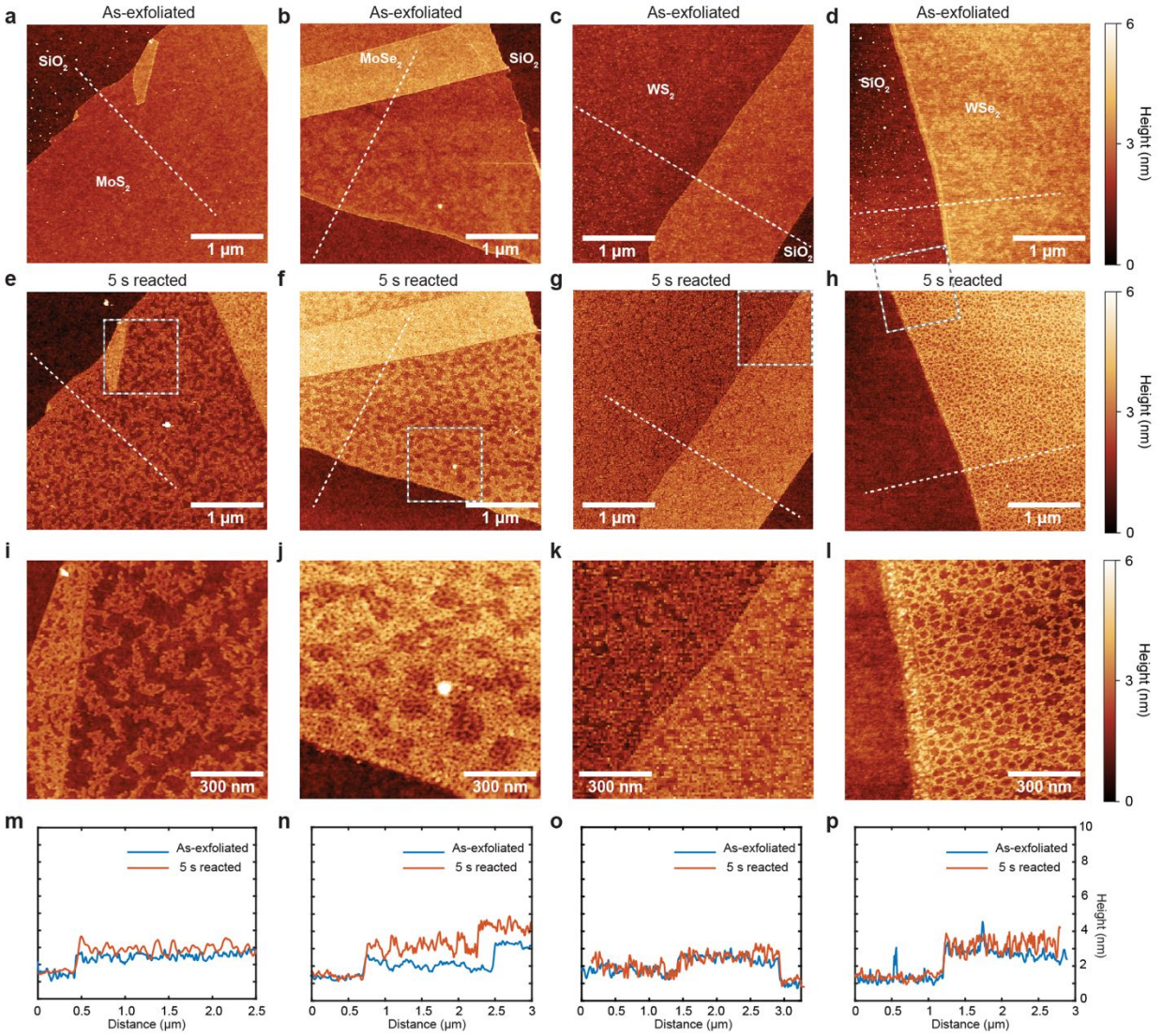

Figure 4. Surface functionalization of TMDCs imaged by atomic force microscopy (AFM). (a)-(d) As-exfoliated flakes of MoS_2, $MoSe_2$, WS_2 and WSe_2. (e)-(h) The flakes shown in (a)-(d) after 5 s functionalization with 10 mM of 4-NBD aqueous solution. (i)-(l) Zoom-in images of areas highlighted with dashed squares shown in (e)-(h). (m)-(p) Height profiles of the lines drawn across the flakes before and after functionalization. (Panels (a), (e), and (i) reprinted with permission from Chu et al.[22] Copyright 2018 American Chemical Society.)

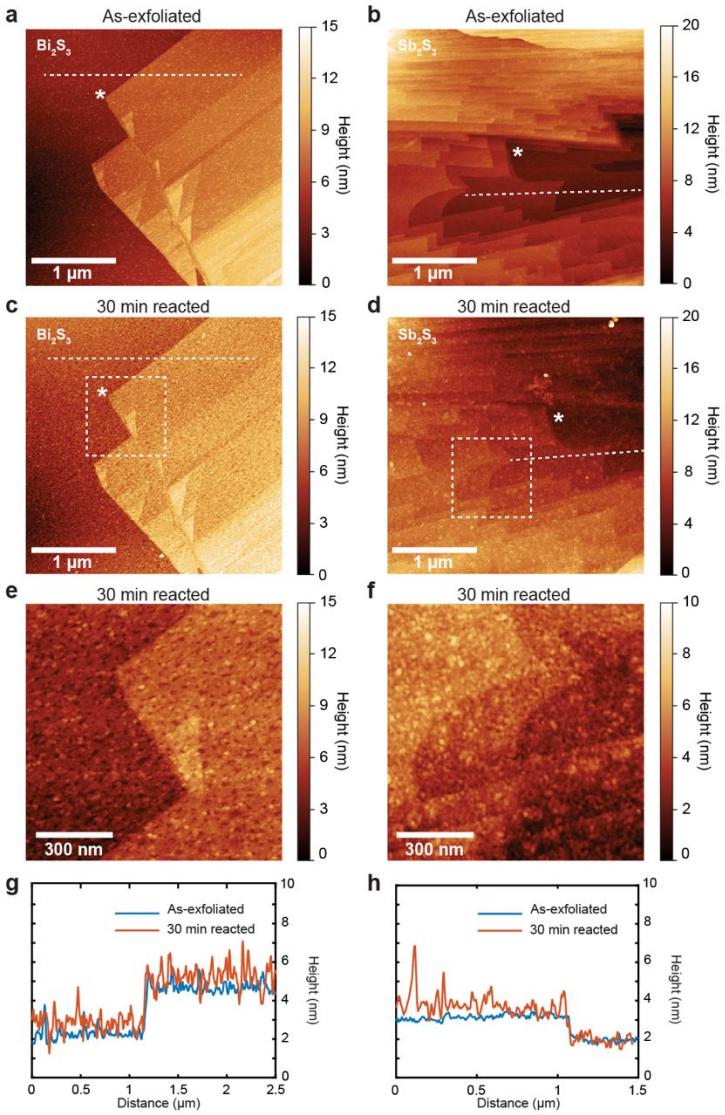

Figure 5. Surface functionalization of PCs imaged by atomic force microscopy (AFM). (a)-(b) As-exfoliated multilayer flakes of Bi_2S_3 and Sb_2S_3. Images are taken in the interiors of multilayer flakes, so the SiO_2/Si substrate is not shown. (c)-(d) The flakes shown in (a)-(b) after 30 min functionalization with 10 mM of 4-NBD aqueous solution. (e)-(f) Zoomed-in images of areas highlighted with dashed squares in (c)-(d). (g)-(h) Height profiles of the dashed lines drawn across the flakes before and after functionalization.

The morphologies of liquid exfoliated samples before and after 4-NBD functionalization were characterized by TEM imaging. Dispersions of nanosheets of TMDCs and PCs were prepared by dropping them onto lacey carbon grids. The samples that were studied were as-dispersed, treated with 4-NBD solution by sonication, and treated without 4-NBD solution by sonication as controls. Representative TEM images of these nanosheets are shown in **Figure 6**. There is relatively little visible change between the functionalized and non-functionalized WS_2 nanosheets as seen in **Figure 6a-c**. The nanosheets are still clearly visible as being quite thin, having different layer thicknesses, and being about 50-100 nm across.

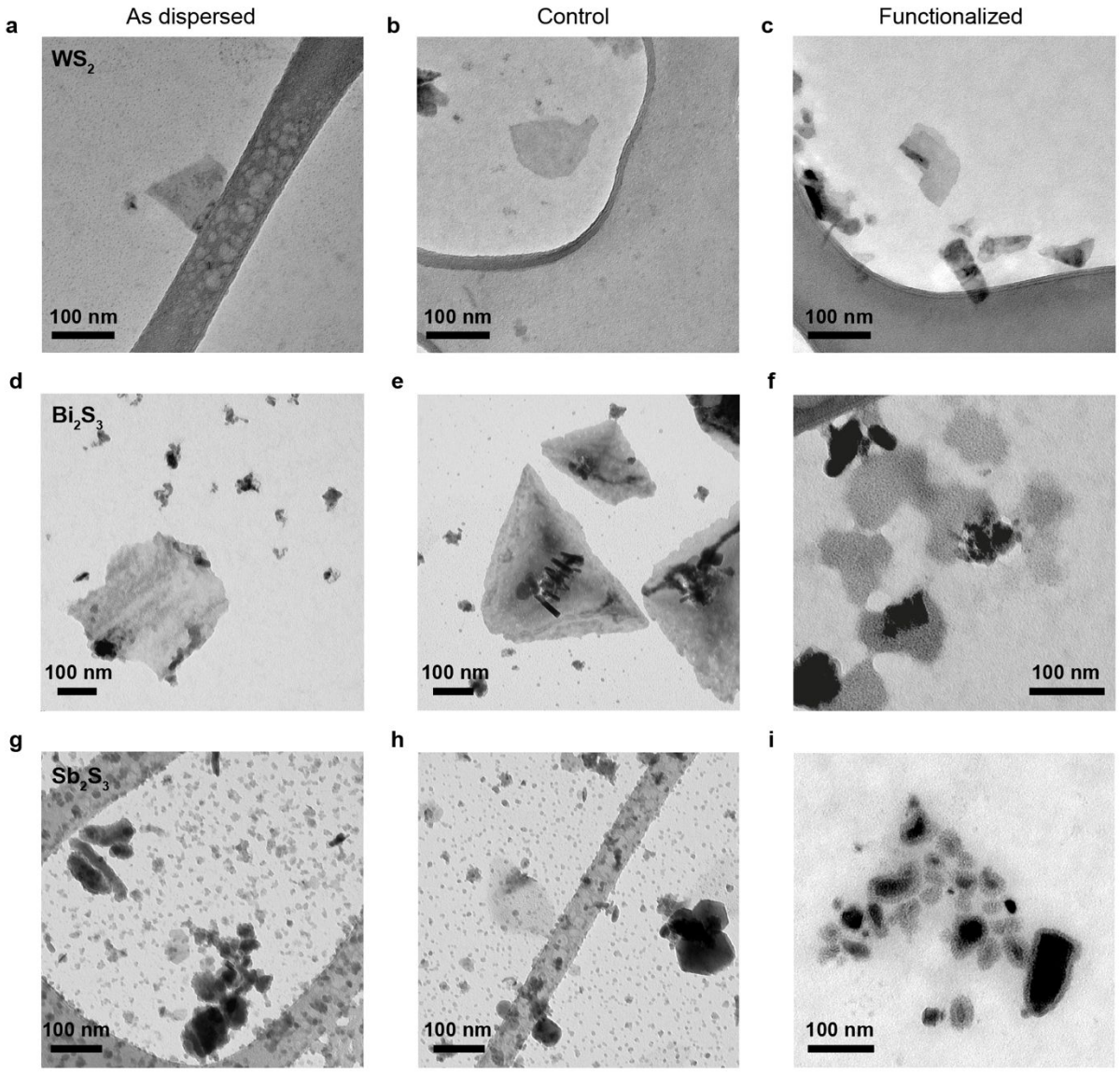

Figure 6. Transmission electron microscopy (TEM) of functionalized nanosheets. (a), (d) and (g) show nanosheets after exfoliation in SDS for WS_2, Bi_2S_3, and Sb_2S_3. (b), (e) and (h) show exfoliated flakes after additional sonication treatment with no 4-NBD to serve as a control. (c), (f) and (i) show exfoliated flakes after additional sonication treatment in the presence of 4-NBD to functionalize them.

For the PCs, a few distinct changes can be seen between functionalized and unfunctionalized samples. For Bi_2S_3, the as-dispersed nanosheets in **Figure 6d** have a distribution of large (a few hundred nanometers across) and small flakes, as do the control nanosheets with additional sonication but no 4-NBD exposure (**Figure 6e**). When the as-dispersed samples are functionalized with 4-NBD, as shown in **Figure 6f**, there are small particles on the surface of the flakes that are observed. We attribute these small particles to similar protrusions that are observed in AFM in **Figure 5e**, suggesting the successful attachment of NP

groups onto the surface of Bi_2S_3. In the case of Sb_2S_3, the as-dispersed control in **Figure 6g** and treated samples without 4-NBD (**Figure 6h**) showed similar morphologies, but the 4-NBD treated samples (**Figure 6i**) seem to have a coating around them, which may be due to a higher degree of functionalization extending into an oligomer formation or surface polymerization regime for these samples since the functionalization time for these materials was 4 h to ensure strong signals in FTIR, while the AFM samples were reacted for 30 min to maintain visibility of the underlying PC nanosheet surface.

Discussion

The combination of spectroscopic and microscopic characterization methods here show the successful covalent functionalization of layered chalcogenide materials. FTIR spectroscopy reveals the successful attachment of nitrophenyl groups on TMDCs and PCs, particularly from the presence of the vibrations from the N-O, C=C, C-S, and C-Se bonds. Similarly from XPS data on MoS_2 and $MoSe_2$, we observe peaks consistent with successful covalent functionalization with the nitrophenyl groups. The TMDC and PC materials do not undergo any significant changes to their intrinsic crystal structures as elucidated by Raman spectroscopy. AFM and TEM imaging show the changes in morphology of the TMDCs and PCs upon functionalization. AFM imaging in particular clearly reveals the formation of small protrusions on the surfaces of all the mechanically exfoliated TMDCs and PCs, consistent with our previous observations for the functionalization of MoS_2.[31,32] These protrusions have a similar height, and are attributed to the nitrophenyl groups attached to the basal planes of the layered chalcogenides. TEM imaging shows the nanosheets from liquid phase dispersion remain well-dispersed and stable upon functionalization, and with some low density features such as particles and overlayers that may correspond to the organic material covalently attached to the PCs. The functionalized materials also remain stable in aqueous dispersions, without noticeable clumping or precipitation.

The proposed reaction mechanism for these materials is briefly discussed here. In our earlier work in Chu et al.[31] we showed for MoS_2 via DFT calculations and experiments using Ar^+ ions to introduce point defects imaged by STM that the functionalization reaction does depend on the presence of existing defects to initiate the reaction. Thus, an otherwise perfect crystal can be fully functionalized with just one initial defect, with the reaction propagating across the surface in a chain-like morphology. Our evidence from Raman, FTIR and AFM imaging suggests that a similar effect may be occurring for the new materials compositions in the current study. That is, the initial layered chalcogenide materials are nearly perfect based on their Raman spectra and the functionalization reaction proceeds by initiating at defects and edges and progresses in chain-like formations which can be seen in AFM images.

This functionalization scheme with diazonium salts is thus compatible with both wafer-scale and solution-based processing of TMDCs and PCs, and can be extended to other chemistries that have been previously used with graphene and MoS_2 to build from the aryl diazonium salts to form composite structures with quantum dots,[53] polymers,[56] and proteins,[31,51] and to induces changes to the electronic properties.[23,49] We anticipate similar changes and applications will be possible for the TMDCd and PCs. That is, we will be

able to exploit the known chemistries that were developed for the earlier materials like graphene and apply them to the TMDCs and PCs.

Conclusions

In conclusion, the functionalization of several compositions of 2D layered chalcogens from the TMDC and PC families has been demonstrated using aryl diazonium chemistry. While our earlier work studied the functionalization of only MoS_2 in detail, the present work demonstrates that this chemistry can readily be expanded to many other 2D layered chalcogens, in both mechanically exfoliated flakes and liquid phase dispersions. Thus, we have established that the aryl diazonium chemistry is a generalizable, effective, and broadly applicable approach to covalent functionalization of a diverse range of several compositions of 2D layered chalcogenides. The functionalized materials are characterized by a combination of spectroscopic and microscopic methods to show the presence of nitrophenyl groups attached to the surfaces of the TMDC materials MoS_2, $MoSe_2$, WS_2, and WSe_2, and the PC materials Bi_2S_3 and Sb_2S_3. This work provides a valuable chemical tool for the modification and application of layered chalcogenides, and opens the door to further chemistries that will expand the functionalities of these low-dimensional materials.

Conflicts of Interest

There are no conflicts of interest to declare.

Acknowledgements

We acknowledge the use of facilities within the Eyring Materials Center at Arizona State University, supported in part by NSF grant NNCI-ECCS-1542160. We also thank Prof. Hao Yan for use of his AFM and Raman spectroscopy systems. We also acknowledge support from NSF grants DMR-1610153 and EEC-1449500.

Electronic Supporting Information

Electronic supplementary information (ESI) contains Raman spectra of mechanically exfoliated samples of all the materials before and after functionalization.

Table of Contents Figure

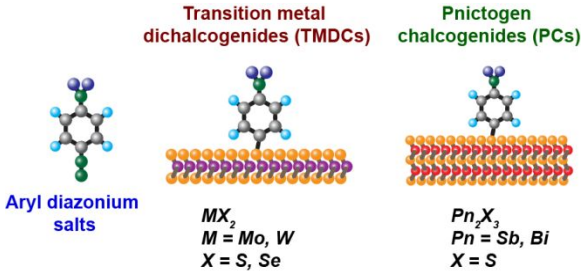

The covalent functionalization of the surfaces of transition metal dichalcogenide and pnictogen chalcogenide materials is demonstrated using aryl diazonium chemistry.

References

1. Q.H. Wang, K. Kalantar-Zadeh, A. Kis, J.N. Coleman, M.S. Strano. Electronics and optoelectronics of two-dimensional transition metal dichalcogenides. *Nat. Nanotechnol.* **2012**, 7 (11), 699–712.
2. M. Chhowalla, H.S. Shin, G. Eda, et al. The chemistry of two-dimensional layered transition metal dichalcogenide nanosheets. *Nat. Chem.* **2013**, 5 (4), 263–275.
3. D. Jariwala, V.K. Sangwan, L.J. Lauhon, T.J. Marks, M.C. Hersam. Emerging Device Applications for Semiconducting Two-Dimensional Transition Metal Dichalcogenides. *ACS Nano* **2014**, 8 (2), 1102–1120.
4. S. Manzeli, D. Ovchinnikov, D. Pasquier, O.V. Yazyev, A. Kis. 2D transition metal dichalcogenides. *Nat. Rev. Mater.* **2017**, 2 (8), 17033.
5. W. Choi, N. Choudhary, G.H. Han, et al. Recent development of two-dimensional transition metal dichalcogenides and their applications. *Mater. Today* **2017**, 20 (3), 116–130.
6. K.F. Mak, J. Shan. Photonics and optoelectronics of 2D semiconductor transition metal dichalcogenides. *Nat. Photonics* **2016**, 10 (4), 216–226.
7. R. Lv, J.A. Robinson, R.E. Schaak, et al. Transition Metal Dichalcogenides and Beyond: Synthesis, Properties, and Applications of Single- and Few-Layer Nanosheets. *Acc. Chem. Res.* **2015**, 48 (1), 56–64.
8. J.-Y. Hwang, Y.-M. Kim, K.H. Lee, H. Ohta, S.W. Kim. Te Monolayer-Driven Spontaneous van der Waals Epitaxy of Two-dimensional Pnictogen Chalcogenide Film on Sapphire. *Nano Lett.* **2017**, 17 (10), 6140–6145.
9. C. García-Mendoza, S. Oros-Ruiz, S. Ramírez-Rave, et al. Synthesis of Bi_2S_3 nanorods supported on ZrO_2 semiconductor as an efficient photocatalyst for hydrogen production under UV and visible light. *J. Chem. Technol. Biotechnol.* **2017**, 92 (7), 1503–1510.
10. Y. Luo, H. Chen, X. Li, et al. Wet chemical synthesis of Bi_2S_3 nanorods for efficient photocatalysis. *Mater. Lett.* **2013**, 105, 12–15.

11. M.B. Sigman, B.A. Korgel. Solventless Synthesis of Bi_2S_3 (Bismuthinite) Nanorods, Nanowires, and Nanofabric. *Chem. Mater.* **2005**, 17 (7), 1655–1660.
12. S. Wen, J. Zhao, Y. Zhao, T. Xu, J. Xu. Reduced graphene oxide (RGO) decorated Sb_2S_3 nanorods as anode material for sodium-ion batteries. *Chem. Phys. Lett.* **2019**, 716, 171–176.
13. F. Lu, R. Li, Y. Li, et al. Improving the Field-Effect Performance of Bi_2S_3 Single Nanowires by an Asymmetric Device Fabrication. *ChemPhysChem* **2015**, 16 (1), 99–103.
14. Y. Yu, C.H. Jin, R.H. Wang, Q. Chen, L.-M. Peng. High-Quality Ultralong Bi_2S_3 Nanowires: Structure, Growth, and Properties. *J. Phys. Chem. B* **2005**, 109 (40), 18772–18776.
15. N. Dhar, N. Syed, M. Mohiuddin, et al. Exfoliation Behavior of van der Waals Strings: Case Study of Bi_2S_3. *ACS Appl. Mater. Interfaces* **2018**, 10 (49), 42603–42611.
16. R.M. Clark, J.C. Kotsakidis, B. Weber, et al. Exfoliation of Quasi-Stratified Bi_2S_3 Crystals into Micron-Scale Ultrathin Corrugated Nanosheets. *Chem. Mater.* **2016**, 28 (24), 8942–8950.
17. Y. Guo, Q. Zhao, Z. Yao, et al. Efficient mixed-solvent exfoliation of few-quintuple layer Bi_2S_3 and its photoelectric response. *Nanotechnology* **2017**, 28 (33), 335602.
18. H. Hou, M. Jing, Z. Huang, et al. One-Dimensional Rod-Like Sb_2S_3-Based Anode for High-Performance Sodium-Ion Batteries. *ACS Appl. Mater. Interfaces* **2015**, 7 (34), 19362–19369.
19. S. Ito, S. Tanaka, K. Manabe, H. Nishino. Effects of Surface Blocking Layer of Sb_2S_3 on Nanocrystalline TiO_2 for $CH_3NH_3PbI_3$ Perovskite Solar Cells. *J. Phys. Chem. C* **2014**, 118 (30), 16995–17000.
20. S.-J. Moon, Y. Itzhaik, J.-H. Yum, et al. Sb_2S_3-Based Mesoscopic Solar Cell using an Organic Hole Conductor. *J. Phys. Chem. Lett.* **2010**, 1 (10), 1524–1527.
21. T. Kuila, S. Bose, A.K. Mishra, et al. Chemical functionalization of graphene and its applications. *Prog. Mater. Sci.* **2012**, 57 (7), 1061–1105.
22. G.L.C. Paulus, Q.H. Wang, M.S. Strano. Covalent Electron Transfer Chemistry of Graphene with Diazonium Salts. *Acc. Chem. Res.* **2013**, 46 (1), 160–170.
23. A. Kaplan, Z. Yuan, J.D. Benck, et al. Current and future directions in electron transfer chemistry of graphene. *Chem. Soc. Rev.* **2017**, 46 (15), 4530–4571.
24. K. Kalantar-zadeh, J.Z. Ou, T. Daeneke, et al. Two-Dimensional Transition Metal Dichalcogenides in Biosystems. *Adv. Funct. Mater.* **2015**, 25 (32), 5086–5099.
25. S.S. Chou, M. De, J. Kim, et al. Ligand Conjugation of Chemically Exfoliated MoS_2. *J. Am. Chem. Soc.* **2013**, 135 (12), 4584–4587.
26. T.W. Kang, J. Han, S. Lee, et al. 2D transition metal dichalcogenides with glucan multivalency for antibody-free pathogen recognition. *Nat. Commun.* **2018**, 9 (1), 2549.
27. S. Karunakaran, S. Pandit, B. Basu, M. De. Simultaneous Exfoliation and Functionalization of 2H-MoS2 by Thiolated Surfactants: Applications in Enhanced Antibacterial Activity. *J. Am. Chem. Soc.* **2018**, 140 (39), 12634–12644.

28. X.-W. Huang, J.-J. Wei, T. Liu, et al. Silk fibroin-assisted exfoliation and functionalization of transition metal dichalcogenide nanosheets for antibacterial wound dressings. *Nanoscale* **2017**, 9 (44), 17193–17198.
29. S. Yang, M. Hua, L. Shen, et al. Phosphonate and carboxylic acid co-functionalized MoS2 sheets for efficient sorption of uranium and europium: Multiple groups for broad-spectrum adsorption. *J. Hazard. Mater.* **2018**, 354, 191–197.
30. S. Hong, H. Im, Y.K. Hong, et al. n-Type Doping Effect of CVD-Grown Multilayer MoSe2 Thin Film Transistors by Two-Step Functionalization. *Adv. Electron. Mater.* **2018**, 4 (12), 1800308.
31. X.S. Chu, A. Yousaf, D.O. Li, et al. Direct Covalent Chemical Functionalization of Unmodified Two-Dimensional Molybdenum Disulfide. *Chem. Mater.* **2018**, 30 (6), 2112–2128.
32. D.O. Li, X.S. Chu, Q.H. Wang. Reaction kinetics for the covalent functionalization of two-dimensional MoS_2 by aryl diazonium salts. *Langmuir* **2019**.
33. Q.H. Wang, Z. Jin, K.K. Kim, et al. Understanding and controlling the substrate effect on graphene electron-transfer chemistry via reactivity imprint lithography. *Nat. Chem.* **2012**, 4 (9), 724.
34. Q.H. Wang, C.-J. Shih, G.L. Paulus, M.S. Strano. Evolution of physical and electronic structures of bilayer graphene upon chemical functionalization. *J. Am. Chem. Soc.* **2013**, 135 (50), 18866–18875.
35. C.R. Ryder, J.D. Wood, S.A. Wells, et al. Covalent functionalization and passivation of exfoliated black phosphorus via aryl diazonium chemistry. *Nat. Chem.* **2016**, 8 (6), 597–602.
36. J.L. Bahr, J. Yang, D.V. Kosynkin, et al. Functionalization of Carbon Nanotubes by Electrochemical Reduction of Aryl Diazonium Salts: A Bucky Paper Electrode. *J. Am. Chem. Soc.* **2001**, 123 (27), 6536–6542.
37. K.C. Knirsch, N.C. Berner, H.C. Nerl, et al. Basal-Plane Functionalization of Chemically Exfoliated Molybdenum Disulfide by Diazonium Salts. *ACS Nano* **2015**, 9 (6), 6018–6030.
38. D. Voiry, A. Goswami, R. Kappera, et al. Covalent functionalization of monolayered transition metal dichalcogenides by phase engineering. *Nat. Chem.* **2015**, 7 (1), 45–49.
39. J. Wang, C. Ma, X. Mu, et al. Construction of multifunctional MoSe2 hybrid towards the simultaneous improvements in fire safety and mechanical property of polymer. *J. Hazard. Mater.* **2018**, 352, 36–46.
40. Z. Chen, L. Guo, H. Yan, et al. Amino functionalization of graphene/graphene-like MoSe2 hybrids as lubricant additives for bismaleimide composites: Preparation, mechanical and tribological properties. *Compos. Part B Eng.* **2019**, 161, 263–271.
41. S. Lei, X. Wang, B. Li, et al. Surface functionalization of two-dimensional metal chalcogenides by Lewis acid–base chemistry. *Nat. Nanotechnol.* **2016**, 11 (5), 465–471.
42. E.D. Grayfer, M.N. Kozlova, V.E. Fedorov. Colloidal 2D nanosheets of MoS2 and other transition metal dichalcogenides through liquid-phase exfoliation. *Adv. Colloid Interface Sci.* **2017**, 245, 40–61.

43. S. Manjunatha, S. Rajesh, P. Vishnoi, C.N.R. Rao. Reaction with organic halides as a general method for the covalent functionalization of nanosheets of 2D chalcogenides and related materials. *J. Mater. Res.* **2017**, 32 (15), 2984–2992.
44. P. Vishnoi, A. Sampath, U.V. Waghmare, C.N.R. Rao. Covalent Functionalization of Nanosheets of MoS2 and MoSe2 by Substituted Benzenes and Other Organic Molecules. *Chem. – Eur. J.* **2017**, 23 (4), 886–895.
45. F.P. Ramanery, A.A.P. Mansur, H.S. Mansur, S.M. Carvalho, M.C. Fonseca. Biocompatible Fluorescent Core-Shell Nanoconjugates Based on Chitosan/Bi2S3 Quantum Dots. *Nanoscale Res. Lett.* **2016**, 11 (1), 187.
46. A.A.P. Mansur, F.P. Ramanery, L.C. Oliveira, H.S. Mansur. Carboxymethyl chitosan functionalization of Bi2S3 quantum dots: Towards eco-friendly fluorescent core-shell nanoprobes. *Carbohydr. Polym.* **2016**, 146, 455–466.
47. R. Dou, Z. Du, T. Bao, et al. The polyvinylpyrrolidone functionalized rGO/Bi2S3 nanocomposite as a near-infrared light-responsive nanovehicle for chemo-photothermal therapy of cancer. *Nanoscale* **2016**, 8 (22), 11531–11542.
48. Y. Wang, Y. Wu, Y. Liu, et al. BSA-Mediated Synthesis of Bismuth Sulfide Nanotheranostic Agents for Tumor Multimodal Imaging and Thermoradiotherapy. *Adv. Funct. Mater.* **2016**, 26 (29), 5335–5344.
49. C.-J. Shih, Q.H. Wang, Z. Jin, et al. Disorder Imposed Limits of Mono- and Bilayer Graphene Electronic Modification Using Covalent Chemistry. *Nano Lett.* **2013**, 13 (2), 809–817.
50. D. Nečas, P. Klapetek. Gwyddion: an open-source software for SPM data analysis. *Cent. Eur. J. Phys.* **2012**, 10 (1), 181–188.
51. Q.H. Wang, Z. Jin, K.K. Kim, et al. Understanding and controlling the substrate effect on graphene electron-transfer chemistry via reactivity imprint lithography. *Nat. Chem.* **2012**, 4 (9), 724–732.
52. J. Greenwood, T.H. Phan, Y. Fujita, et al. Covalent Modification of Graphene and Graphite Using Diazonium Chemistry: Tunable Grafting and Nanomanipulation. *ACS Nano* **2015**, 9 (5), 5520–5535.
53. Y. Liang, J.E. Thorne, B.A. Parkinson. Controlling the Electronic Coupling between CdSe Quantum Dots and Thiol Capping Ligands via pH and Ligand Selection. *Langmuir* **2012**, 28 (30), 11072–11077.
54. G. Eda, H. Yamaguchi, D. Voiry, et al. Photoluminescence from Chemically Exfoliated MoS_2. *Nano Lett.* **2011**, 11 (12), 5111–5116.
55. F.M. Koehler, A. Jacobsen, K. Ensslin, C. Stampfer, W.J. Stark. Selective Chemical Modification of Graphene Surfaces: Distinction Between Single- and Bilayer Graphene. *Small* **2010**, 6 (10), 1125–1130.
56. J. Liu, L. Cui, N. Kong, C.J. Barrow, W. Yang. RAFT controlled synthesis of graphene/polymer hydrogel with enhanced mechanical property for pH-controlled drug release. *Eur. Polym. J.* **2014**, 50, 9–17.